

# **Nanocrystalline chromium-based coatings deposited by DLI-MOCVD under atmospheric pressure from Cr(CO)<sub>6</sub>**

**A. Douard and F. Maury**

Centre Interuniversitaire de Recherche et d'Ingénierie des Matériaux (CIRIMAT),  
CNRS/INPT/UPS, ENSIACET, 118 route de Narbonne, 31077 Toulouse cedex 4, France

## **Abstract**

Nanocrystalline original Cr-based coatings were grown under atmospheric pressure by Direct Liquid Injection Metal Organic Chemical Vapor Deposition (DLI-MOCVD). The thin films were grown below 450 °C in a cold wall CVD reactor from solutions of Cr(CO)<sub>6</sub> in toluene or THF injected and flash vaporized with or without NH<sub>3</sub> addition prior to the deposition zone. Original nanocrystalline chromium oxycarbide and oxy-carbonitride phases were deposited on stainless steel substrates. The influence of injection parameters and conventional CVD conditions have been investigated on the main chemical, physical and structural characteristics of the coatings, as deduced from XRD, SEM, and EPMA analyses.

**Keywords:** DLI-CVD; MOCVD; Chromium-based coatings; Atmospheric deposition process

1. Introduction
  2. Experimental
  3. Results and discussion
    - 3.1. Choice of the solvent
    - 3.2. Growth with Cr(CO)<sub>6</sub>/THF
    - 3.3. Growth with Cr(CO)<sub>6</sub>/toluene
    - 3.4. Growth with Cr(CO)<sub>6</sub>/toluene/NH<sub>3</sub>
  4. Conclusion
- References

# **1. Introduction**

Atmospheric metalorganic chemical vapor deposition (MOCVD) is an attractive process for large scale deposition of protective metallurgical coatings. Among the advantages, high vacuum technology is not required, which will reduce servicing costs and stop periods. Moreover, the use of metalorganic compounds as molecular precursor decreases the deposition temperature compared with the well known halide precursors and allows deposition on metal pieces while preserving the base properties of the substrates. Metalorganic compounds are well known for their decomposition at low temperature and subsequently for their poor thermal stability. As a result, the heating in conventional vaporization bubblers (or saturators) for a long period leads to the premature decomposition of the precursor prior to the reactor. Furthermore, the most part of the metalorganic compounds are solids and when the carrier gas passes through the powder to deliver the precursor vapor, an agglomeration is frequently observed, making difficult an accurate control of the precursor flow rate. To overcome this problem, several solutions have been proposed based on the flash vaporization (i) of precursor powder [1], (ii) of an aerosol produced by an ultrasonic technique (AACVD) [2], (iii) of a pulsed direct liquid injection precursor solution (DLI-CVD) [3] and [4]. In DLI-CVD, previous works report the growth of simple oxide layers [5], multicomponent coatings [6], oxide multilayers [7], oxide superlattices [8], noble metal films like Ir [9], Cu [10], Ag [11] and also (Al, Ti)N diffusion barrier [12]. It is noteworthy that most of these DLI-CVD processes operated under reduced pressure and were developed for microelectronic applications.

In this paper, we report for the first time the deposition of nanocrystalline Cr-based metallurgical coatings by DLI-CVD under atmospheric pressure. Cr-based coatings are good candidates for the steel protection owing to their good resistance to wear and corrosion and their high hardness. Coatings in the Cr–C–N system were previously reported by conventional MOCVD operating generally under low pressure [13], [14] and [15]. In the present paper,  $\text{Cr}(\text{CO})_6$  was chosen as chromium source because of its commercial availability, its low cost, its good stability under ambient conditions and its decomposition at low temperature. We study the thermal decomposition of a DLI solution of  $\text{Cr}(\text{CO})_6$  either in toluene or THF at 350–450 °C under atmospheric pressure with or without  $\text{NH}_3$  addition prior to the deposition zone. We discuss on the influence of conventional CVD conditions like the precursor molar

fraction and the deposition temperature on the morphology and the growth rate of the films and we also study the role of specific DLI-CVD conditions like the presence of the solvent and the injection conditions on the main characteristics of the as-deposited coatings.

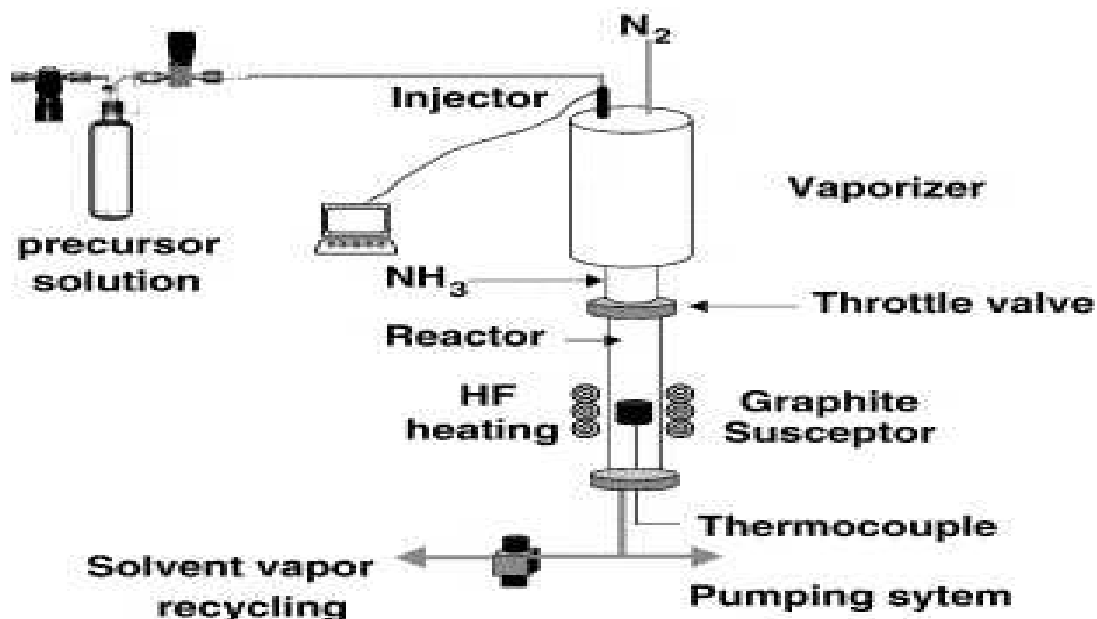
## **2. Experimental**

Chromium oxides  $\text{CrO}(\text{C})$ , chromium oxycarbides  $\text{Cr}_x\text{C}_y\text{O}_z$  and chromium oxy-carbonitrides  $\text{CrN}_x\text{O}_y\text{C}_z$  films were deposited by DLI-CVD using a solution of  $\text{Cr}(\text{CO})_6$  either in toluene or tetrahydrofuran (THF). The liquid source reagent, maintained at room temperature and pressurized under 3 bar of  $\text{N}_2$  atmosphere, was introduced in micro-amounts by means of a modified automotive injector in the evaporator under atmospheric pressure and heated at 250 °C. The opening time of the injector, its needle frequency and the pulse number are accurately controlled by monitoring using a computer. The amount of injected solution increases with the injection frequency, the injector opening time, the differential pressure between the liquid pressurized vessel and the vaporization chamber, and depends also on the viscosity of the precursor solution. Flash vaporization of small droplets occurs in the evaporator then solvent and precursor vapors are transported using  $\text{N}_2$  as carrier gas (5000  $\text{cm}^3/\text{min}$ ) from the injector nozzle zone to the substrates through the vertical evaporator and the CVD reactor. Under atmospheric pressure, the vaporizer must be held at least at the boiling temperature of the used solvent. Because the volume of the droplets depends on the injector and also on the pressure difference between the injector and the vaporizer, under atmospheric pressure, an efficient flash evaporation requires opening times ( $< 0.5$  ms) shorter than those used in low pressure DLI-CVD processes.

The evaporator is co-axially linked to a vertical cold wall CVD Pyrex glass reactor. The substrates (Si(100) wafer and 304L stainless steel small plates) were supported by a SiC passivated graphite susceptor heated by HF induction and placed 5 cm below the evaporator bottom. To avoid any condensation of the precursor and of the solvent during the transport of the reactive vapor to the substrate, the  $\text{N}_2$  carrier gas is heated at a temperature close to that of the vaporization chamber. To prevent interactions between the substrates and non vaporized droplets, a chicane is placed at the bottom of the vaporizer. After vacuum purge for 24 h, the

CVD reactor was pressurized with nitrogen to 1 atm prior to the deposition. The DLI-CVD set-up is schematized in [Fig. 1](#).

Fig. 1. Sketch of the DLI-CVD reactor operating under atmospheric pressure.



The structure of the coatings was determined by X-ray diffraction (Cu K $\alpha$ ). The average crystallite size was determined using the Scherrer's formula from the width at half maximum of the (200) peak of the fcc structure of the deposited film. The chemical composition was analyzed by electron probe microanalysis (EPMA) and the surface morphology was examined by SEM.

### **3. Results and discussion**

#### **3.1. Choice of the solvent**

Liquid solution feeding system is very suitable and promising in MOCVD to evaporate solid metalorganic precursors sensitive to thermal decomposition, occurring sometimes during their vaporization from a bubbler and the vapor transport in heated pipes.

Furthermore an accurate and repeatable control of the precursor flow rate is required in the CVD reactor. Organic solvents are commonly employed to make soluble metalorganic compounds. But the choice of adequate solvents is relatively delicate because not only several parameters like the physical and chemical properties must be taken into consideration but also toxicity, cost, commercial availability, safety, environmentally friendly. Consequently, selection of the solvent is a key point of the process. The solvent must not react with the precursor and the corresponding saturation concentration in precursor must be as high as possible in order to deliver high flow rates of precursor in the CVD reactor (0.01 mol/l is a common value in the literature). For  $\text{Cr}(\text{CO})_6$ , saturation concentrations in toluene and in THF were determined at respectively 0.02 mol/l and 0.07 mol/l. We notice that the saturation concentration rises with the dipolar moment; so polar solvents like THF are suitable for  $\text{Cr}(\text{CO})_6$ . The relatively high flow rate of solvent vapor could lead to the incorporation of undesirable elements like carbon or oxygen in the coating originating from the solvent. [Table 1](#) sums up the experimental runs and the main results of the structural and chemical characterizations of typical samples.

Table 1.

DLI-CVD conditions and principal characteristics of the  $\text{CrC}_x\text{O}_y$  and  $\text{CrN}_x\text{O}_y\text{C}_z$  coatings grown under atmospheric pressure using  $\text{Cr}(\text{CO})_6$  as precursor (the opening time was maintained constant at 0.5 ms)

Run no.	Deposition temperature (°C)	Gaseous atmosphere	Frequency (Hz)	$x_R / x_p^{(a)}$	$x_p$ (ppm)	XRD	Crystal lite size (Å)	Growth rate (µm/h)	Composition
1	350	$\text{N}_2 + \text{THF}$	4	0	649	fcc CrCO	25	1.3	$\text{Cr}_{0.54}\text{O}_{0.31}\text{C}_{0.15}$
2	350	$\text{N}_2 + \text{THF}$	4	0	98	fcc CrCO	27	0.7	$\text{Cr}_{0.43}\text{O}_{0.40}\text{C}_{0.17}$
3	350	$\text{N}_2 + \text{toluene}$	4	0	47	fcc CrO	33	0.10	$\text{Cr}_{0.48}\text{O}_{0.47}\text{C}_{0.05}$
4	400	$\text{N}_2 + \text{toluene}$	4	0	52	fcc CrCO	16	0.12	$\text{Cr}_{0.51}\text{O}_{0.30}\text{C}_{0.18}$
5	450	$\text{N}_2 + \text{toluene}$	4	0	50	Unknown structure	–	0.18	$\text{Cr}_{0.57}\text{O}_{0.19}\text{C}_{0.25}$
6	400	$\text{N}_2 + \text{toluene}$	10	0	137	fcc CrCO	9	0.33	$\text{Cr}_{0.59}\text{O}_{0.24}\text{C}_{0.1}$

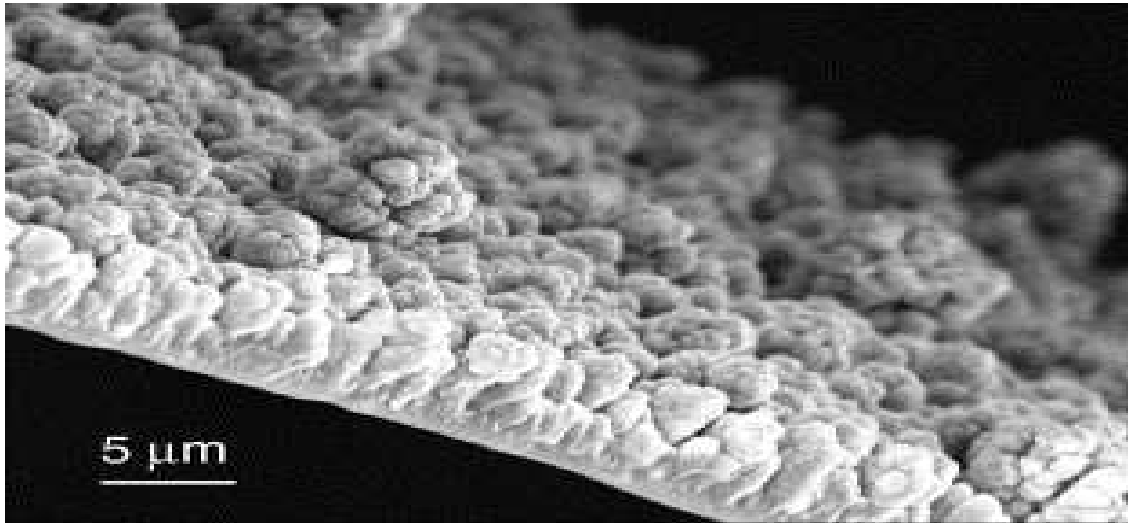
Run no.	Deposition temperature (°C)	Gaseous atmosphere	Frequency (Hz)	$x_R / x_p^{(a)}$	$x_p$ (ppm)	XRD	Crystal size (Å)	Growth rate (µm/h)	Composition
									6
7	350	N <sub>2</sub> + toluene	4	0	226	fcc CrCO + Cr <sub>3</sub> O <sub>4</sub>	36	0.25	Cr <sub>0.37</sub> O <sub>0.43</sub> C <sub>0.20</sub>
8	350	N <sub>2</sub> + toluene + NH <sub>3</sub>	4	1150	51	Amorphous	–	–	Cr <sub>0.31</sub> O <sub>0.36</sub> N <sub>0.22</sub> C <sub>0.11</sub>
9	400	N <sub>2</sub> + toluene + NH <sub>3</sub>	4	1190	50	fcc CrNOC	66	0.10	Cr <sub>0.24</sub> O <sub>0.36</sub> N <sub>0.26</sub> C <sub>0.13</sub>

(a) Ratio between mole fraction of reactive gas ( $x_R$ ) and precursor mole fraction ( $x_p$ ).

### 3.2. Growth with Cr(CO)<sub>6</sub>/THF

The films obtained under N<sub>2</sub> atmosphere with a solution of Cr(CO)<sub>6</sub> in THF are chromium oxycarbides (CrC<sub>x</sub>O<sub>y</sub>). The XRD patterns of these coatings are similar to those reported in the ASTM card files [16]. They exhibit a dull-gray appearance, a relatively high surface roughness and a poor adherence on Si(100). SEM micrographs reveal a rough, nodular and porous surface morphology, constituted of cauliflower-like grains with an average grain size of a few micrometers (Fig. 2). The columnar growth is clearly observed on cross section of a scale detached from the silicon substrate. The growth rate is relatively high and increases from 0.7 µm/h (run 2) to 1.3 µm/h (run 1) by increasing the precursor molar fraction ( $x_p$ ). The growth is probably limited by the feeding of the precursor (diffusion growth regime) but further experiments are required before to conclude. The surface morphology is not better, i.e. the coatings are still porous, with a low value of  $x_p$  obtained either by increasing the N<sub>2</sub> carrier gas flow rate or by decreasing the precursor concentration in the THF solution. The film compositions determined by EPMA are Cr<sub>0.54</sub>O<sub>0.31</sub>C<sub>0.15</sub> for run 1 and Cr<sub>0.43</sub>O<sub>0.40</sub>C<sub>0.17</sub> for run 2. As a result, no significant influence of the precursor molar fraction on the coating composition in carbon was found.

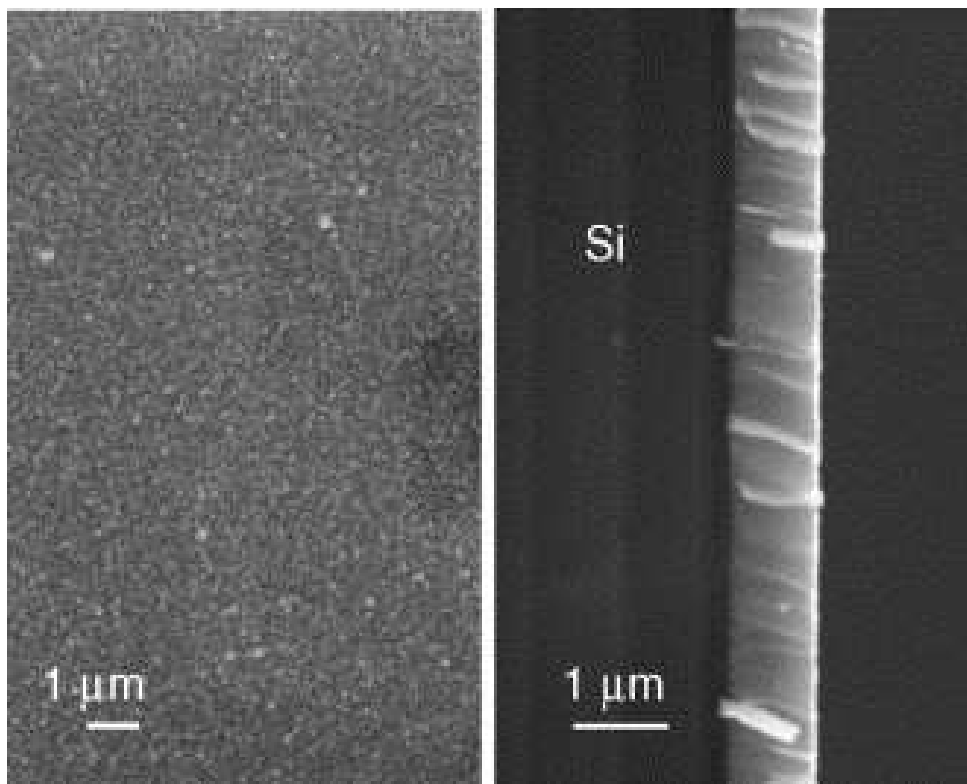
Fig. 2. Surface morphology and cross section of a scale from a CrC<sub>x</sub>O<sub>y</sub> coating on Si(100) grown under N<sub>2</sub> atmosphere with a solution of Cr(CO)<sub>6</sub> in THF (run 1).



### 3.3. Growth with $\text{Cr}(\text{CO})_6$ /toluene

The films obtained under  $\text{N}_2$  atmosphere with a solution of  $\text{Cr}(\text{CO})_6$  in toluene are chromium oxycarbides ( $\text{CrC}_x\text{O}_y$ ) with a variable carbon content depending on the growth conditions ([Table 1](#)). Coatings from runs 3 to 5 exhibit a mirror like appearance with a very smooth surface morphology and a high compactness as shown on the SEM micrograph in [Fig. 3](#). In the early stages of the growth, a thin colored layer is first observed then the coating becomes gray metallic.

Fig. 3. Surface morphology on 304L stainless steel (left) and cross section on Si(100) (right) of a  $\text{CrC}_x\text{O}_y$  coating grown under  $\text{N}_2$  atmosphere with a solution of  $\text{Cr}(\text{CO})_6$  in toluene (run 3).

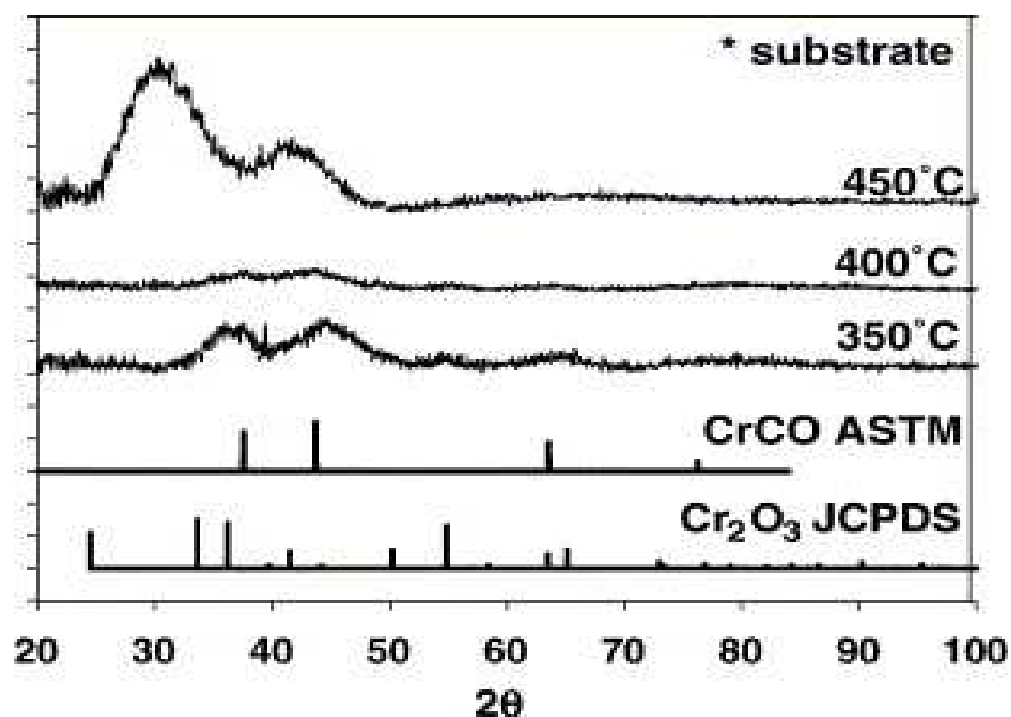


A series of three samples was prepared by increasing the deposition temperature from 350 to 450 °C (runs 3–5). Coatings grown at 350 °C are essentially chromium oxide with a low carbon contamination as given by EPMA data ( $\text{Cr}_{0.48}\text{O}_{0.47}\text{C}_{0.05}$ ). XRD diagrams exhibit broad diffraction peaks which give evidence for a nanocrystalline structure with crystallite mean size of 33 Å. The crystalline phase seems to exhibit an fcc type structure similar to those previously reported for chromium oxides with a Cr : O ratio close to 1 : 1 [17]. This is consistent with the composition found for the run 3. By increasing the deposition temperature to 400 °C, XRD diagrams show a decrease of the peak intensity and of the crystallite sizes, revealing an amorphous transition. The carbon content of the coatings increases with the deposition temperature which may explain this amorphization. For a deposition temperature of 450 °C, XRD pattern of  $\text{CrC}_x\text{O}_y$  coatings exhibit a nanocrystalline structure which is



different from the structure observed at 350 °C and does not exhibit the features of Cr<sub>2</sub>O<sub>3</sub> (Fig. 4).

Fig. 4. XRD diagrams of CrC<sub>x</sub>O<sub>y</sub> coatings grown under N<sub>2</sub> atmosphere with a solution of Cr(CO)<sub>6</sub> in toluene at different increasing deposition temperature. XRD patterns of CrCO [ASTM] and Cr<sub>2</sub>O<sub>3</sub> [JCPDS] are also given for comparison.



In this DLI-CVD process, the influence of the solvent is clearly seen by comparing coatings grown under the same conditions using THF (run 2) and toluene (run 3). In the last case, C content is very low indicating that toluene is more thermally stable than THF. Obviously a part of this incorporated carbon may come from the carbonyl ligands of the precursor. THF and toluene thermal decompositions have only been studied previously at high temperature and under vacuum and a higher activation energy was reported for the thermal decomposition of toluene [18] and [19]. This fact could explain the higher contamination of carbon in coatings grown from a solution of Cr(CO)<sub>6</sub> in THF. However, previous DLI-CVD experiments using hydrocarbon solvents like hexane [7], toluene [12] or THF [18] do not report carbon contamination of the coatings due to the solvent at these deposition temperature. But these works dealt with the deposition of oxide materials under oxidizing atmosphere [7]

and [18] or the deposition of noble metals [9]. No clear relationship was found between the toluene of the DLI solution and the carbon incorporation in (Al,Ti)N [12] but the deposition was carried out in the low temperature range 150–350 °C. In our case, toluene could prevent the dissociative adsorption of CO ligands on the growing surface but this mechanism would be efficient principally at low deposition temperature (350 °C). By increasing the deposition temperature above 350 °C, adsorption of toluene becomes negligible in the competition with CO adsorption and, as a result, the C incorporation originating from CO heterogeneous dissociation likely becomes dominant. Partial gas phase decomposition of toluene may also contribute to the increase of the total C content in the coating when the temperature increases (Table 1).

By contrast with THF, mirror-like appearance, fine-grained surface morphology and compact coatings are observed when toluene is used as solvent. On the other hand, increasing the coating temperature does not influence at large extent the growth rate: 0.1 µm/h at 350 °C (run 3) and 0.18 µm/h at 450 °C (run 5). The estimated activation energy is 15.6 kJ/mol, which is a low value characteristic of a diffusion controlled growth process. However, these growth rates are relatively low (for instance to apply the process for on line coating) and the deposition temperature cannot be increased above 550 °C because of the steel substrates. The growth rate can be increased by increasing the precursor mole fraction as demonstrated by the runs 3 (0.10 µm/h for  $x_p = 47$  ppm) and 7 (0.25 µm/h for  $x_p = 226$  ppm). Thin films from run 7 have a dull-gray colour. SEM observations show a surface morphology constituted of small grains with a mean size of 500 nm and a less compact structure than chromium oxycarbide coatings grown with a lower precursor molar fraction. The composition of the coating from run 7 is  $\text{Cr}_{0.37}\text{O}_{0.43}\text{C}_{0.20}$  which indicates the C content increases with the precursor molar fraction for the coating grown at low temperature (350 °C). For deposition temperature higher than 350 °C, the C content seems independent on the mole fraction of  $\text{Cr}(\text{CO})_6$  (comparison between runs 4 and 6 performed at 400 °C). It confirms that the C incorporation is due to different mechanisms depending of the substrate temperature. At 350 °C and for low mole fraction of  $\text{Cr}(\text{CO})_6$ , the dissociative adsorption of the CO ligands would be blocked by the adsorption of toluene but by increasing  $x_p$ , the toluene molecules are displaced from the surface by the precursor molecule, which contributes to increase the C content of the films. At higher temperature and for low values of  $x_p$ , the solvent molecules do not prevent the dissociative adsorption of CO leading for instance to the incorporation of 18 at.% of C at 400

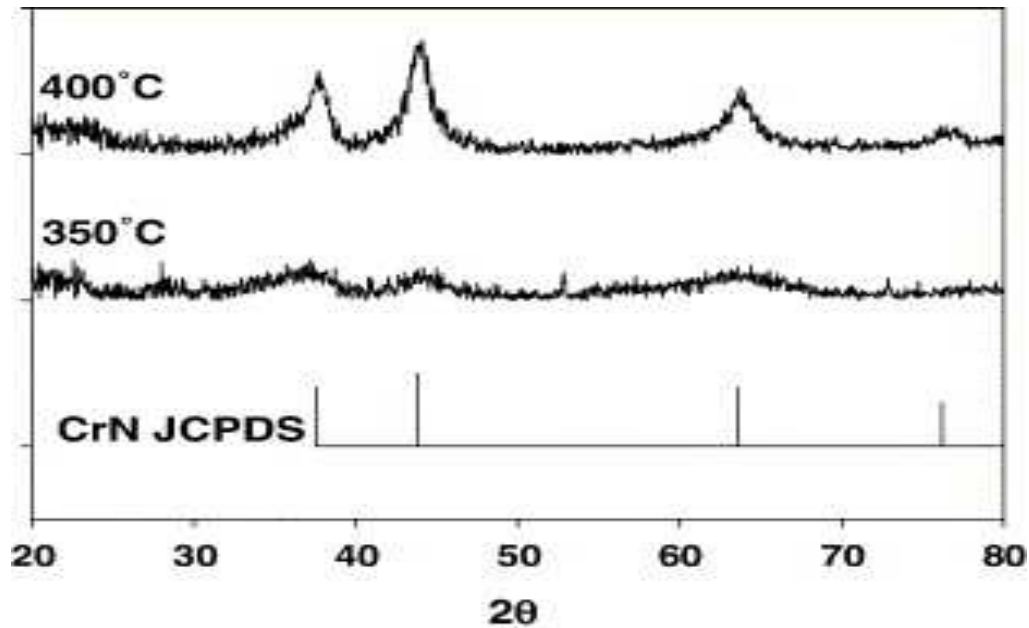
°C (run 4). At the same temperature, the increase of  $x_p$  (run 6) does not increase any more the C content (16 at.%) probably because of the saturation of the adsorption sites.

Coatings from run 6 were obtained at 400 °C like run 5 but with a higher frequency of 10 Hz. XRD diagram exhibits an fcc nanocrystalline structure and the film composition is  $\text{Cr}_{0.59}\text{O}_{0.24}\text{C}_{0.16}$ . SEM observations show a smooth surface morphology and a compact structure. In comparison with run 5 at 400 °C with a 4 Hz frequency, the carbon contamination and the growth rate increase with the frequency. The crystallite size decreases on the other hand. In DLI-CVD, precursor molar fraction could be increased not only by changing the solution concentration but also by increasing the injection frequency, i.e. the precursor flow rate. The corresponding coatings stay like mirror and exhibit a compact structure and a lower crystallite size.

### 3.4. Growth with $\text{Cr}(\text{CO})_6/\text{toluene}/\text{NH}_3$

The films obtained under  $\text{NH}_3$  atmosphere are chromium oxy-carbonitrides ( $\text{CrN}_x\text{O}_y\text{C}_z$ ). These samples have a brightness and yellow-gray color. SEM micrographs show a fine-grained surface morphology, constituted of small grains with a 100 nm mean size and a compact structure. XRD patterns reveal quasi amorphous coatings for a deposition temperature of 350 °C and an fcc CrN-like structure for the coatings deposited at 400 °C (Fig. 5). As-deposited films have a nanocrystalline structure with a crystallite size of 66 Å. During the growth experiment at 350 °C (run 8), a very slow growth was noticed leading to very thin coloured layers. Consequently, the substrate temperature was increased to 400 °C (run 9). At this temperature, the growth rate reaches 0.1  $\mu\text{m}/\text{h}$  which is always too slow for an on line process coating. Adding  $\text{NH}_3$  does not affect significantly the growth rate for a same  $x_p$  at 400 °C (runs 4 and 9).

Fig. 5. XRD diagrams of  $\text{CrN}_x\text{O}_y\text{C}_z$  coatings grown under  $\text{NH}_3$  atmosphere with a solution of  $\text{Cr}(\text{CO})_6$  in toluene at 350 and 400 °C.



The film composition of the run 10 is  $\text{Cr}_{0.31}\text{O}_{0.36}\text{N}_{0.22}\text{C}_{0.11}$ . At this stage, we observe that  $\text{NH}_3$  does not facilitate the carbon and oxygen elimination from the coating to the gas phase as observed in conventional MOCVD [19]. It is probably due to the presence of toluene and this indicates that toluene contributes to the C incorporation into the film. This is confirmed by SIMS profile analyses that reveal, in addition to a uniform distribution of Cr, C, N and O, the presence of hydrogen which likely originates from a thermal cracking of solvent molecules.

## **4. Conclusion**

Chromium oxycarbides  $\text{CrC}_x\text{O}_y$  and chromium oxy-carbonitrides  $\text{CrN}_x\text{O}_y\text{C}_z$  were deposited by DLI-CVD under atmospheric pressure on stainless steel and Si substrates, at temperature as low as 350 °C, using  $\text{Cr}(\text{CO})_6$  as Cr-source either in toluene or THF solution, with or without  $\text{NH}_3$  as reactive gas.  $\text{CrC}_x\text{O}_y$  thin films from the solution of  $\text{Cr}(\text{CO})_6$  in THF exhibit a high growth rate but a rough, porous and undesired morphology for metallurgical coatings. However,  $\text{CrC}_x\text{O}_y$  coatings from the solution in toluene have a mirror-like appearance and exhibit a dense structure. Coatings grown at 350 °C are amorphous then at 400 °C they exhibit a nanocrystalline fcc structure while at 450 °C a structural transformation

is observed. The carbon incorporation is very low at 350 °C but it increases with the deposition temperature and also with the molar precursor fraction under the same DLI-CVD conditions. So both carbonyl ligands of the precursor and toluene are responsible for C incorporation. CrN<sub>x</sub>O<sub>y</sub>C<sub>z</sub> coatings deposited from a DLI solution in toluene with NH<sub>3</sub> at 450 °C exhibit a nanocrystalline fcc structure, a smooth surface and a compact structure. Further characterizations like adherence, nanoindentation and corrosion tests are in progress to study the potentials of these original Cr-based coatings as metallurgical protective coatings. The corresponding growth rate are relatively low to apply these DLI processes for on line deposition because of the low saturation concentration of Cr(CO)<sub>6</sub> in toluene but optimizations on the precursor delivery are currently in progress.

## **References**

- R. Hiskes, S.A. DiCarolis, J.L. Young, S.S. Laderman, R.D. Jacowitz and R.C. Taber, *Appl. Phys. Lett.* 59 (1991) (5), p. 606
- D.A. Edwards, R.M. Harker, M.F. Mahon and K.C. Molloy, *J. Mater. Chem.* 9 (1999), p. 1771.
- A.R. Kaul and B.V. Seleznev, *J. Phys., IV* 3 (1993), p. 375.
- J.P. Sénateur, R. Madar, F. Weiss, O. Thomas, A. Abrutis, French Patent FR 2707671 (1993), European patent EP 730671 (1994), US patent US 945162 (1999).
- F. Felten, J.P. Sénateur, F. Weiss, R. Madar and A. Abrutis, *J. Phys. IV* 5 (1995) (C5), p. 1079.
- A. Abrutis, J.P. Sénateur, F. Weiss, V. Kubilius, V. Bigelytè, Z. Saltylè, B. Vengalis and A. Jukna, *Supercond. Sci. Technol.* 10 (1997), p. 959.
- F. Felten, J.P. Sénateur, M. Labeau, K. Yu-Zhang and A. Abrutis, *Thin Solid Films* 296 (1997), p. 79.

F. Weiss, J. Lindler, J.P. Sénateur, C. Dubourdieu, V. Galindo, M. Audier, A. Abrutis, M. Rosina, K. Fröhlich, W. Haessler, S. Oswald, A. Figueras and J. Santiso, *Surf. Coat. Technol.* 133–134 (2000), p. 191.

J.P. Endle, Y.M. Sun, N. Nguyen, S. Madhukar, R.L. Hance, J.M. White and J.G. Ekerdt, *Thin Solid Films* 388 (2001), p. 126.

C. Marcadal, E. Richard, J. Torres, J. Palleau and R. Madar, *Microelectron. Eng.* 37–38 (1997), p. 97.

L. Gao, P. Härter, Ch. Linsmeier, J. Gstöttner, R. Emling and N. Schmitt-Landsiedel, *Mater. Sci. Semicond. Process.* 7 (2004), p. 331.

J.P. Endle, Y.M. Sun, J. Silverman, N. Nguyen, A.H. Cowley, J.M. White and J.G. Ekerdt, *Thin Solid Films* 385 (2001), p. 66.

F. Schuster, F. Maury, J.F. Nowak and C. Bernard, *Surf. Coat. Technol.* 46 (1991), p. 275.

F. Schuster, F. Maury, N. Pébère, J.F. Nowak and C. Duret-Thual, *Innovation and Technology transfer for Corrosion Control (Proceed 11th Int Corrosion Congress)* vol. 1 (1990), p. 205.

F. Maury, F. Ossola and F. Senocq, *Surf. Coat. Technol.* 133–134 (2000), p. 198.

M. Kmetz, B.J. Tan, W. Willis and S. Suib, *J. Mater. Sci.* 26 (1991), p. 2107.

V. Dufek, F. Petru and V. Brozek, *Monatsh. Chem.* 98 (1967), p. 2424. A.C. Jones, T.J. Leedham, P.J. Wright, M.J. Crosbie, P.A. Lane, D.J. Williams, K.A. Fleeting, D.J. Otway and P. O'Brien, *Chem. Vap. Depos.* 4 (1998) (2), p. 46.

A. Douard and F. Maury, *Surf. Coat. Technol.* 200 (2005) (5–6), p. 1407.

Corresponding author. Tel.: +33 562 885 666; fax: +33 562 885 600.

**Original text : [Elsevier.com](http://www.elsevier.com)**